Proceeding of the 13th National Mechanical Engineering Conference.
2-3 December 1999, Royal Cliff Beach Resort Hotel, South Pattaya, Chonburi.

NANOMETER ORDER PRECISION SERVO POSITIONING SYSTEM USING PIEZO-ELECTRIC ACTUATOR

Unnat Pinsopon

Department of Mechanical Engineering
King Mongkut's Institute of Technology Ladkrabang
Bangkok 10520

ABSTRACT

A nano-metric precision toolpost is designed and fabricated based on a piezo-electric actuator. The toolpost positioning system has single degree of freedom. A capacitive gap sensor with less than 1 nm resolution is used for position feedback. The closed loop controller is implemented using C-language on a 486-IBM PC compatible computer and 16-bit A/D and D/A converter card. The output of the D/A converter is amplified by a specially designed high voltage amplifier Two different classes of control algorithms are tested: 1. Integral, 2. CMAC neural network control algorithms. The closed loop system has about 2 nm positioning accuracy and a bandwidth of about 250 Hz. The CMAC algorithm improved the tracking accuracy compared to PID algorithm. The steady state accuracy of both algorithms were same due to the fact that the accuracy is limited by the sensor resolution in steady state.

INTRODUCTION

There is an increasing number of industrial applications where the positioning accuracy of the motion control system must be in sub-micron range. The accuracy requirements are getting even smaller. It has been reported that single point diamond turning machines are used in machining metal mirrors with less than 100 nm profile accuracy and less than 10 nm surface roughness [Evans, 1991; Ueda et al., 1991]. Similar positioning accuracies are needed in feed-rate control of the hard disk drive machining [Keauskopf, 1984]. Nano-metric positioning accuracy would advance the capabilities of atomic force microscopy (AFM), scanning tunneling microscopy (STM), micro-surgery. The standard drive system in today machine tools is a servo driven lead-screw mechanisms. In contour machining, it is virtually impossible to obtain nano-metric positioning accuracy with lead-screw mechanisms due to the presence of backlash and friction in the drive system from actuation point at the servo motor rotor to the tool position. A so-called *fast tool servo* has been proposed to increase the tool positioning accuracy. The idea is to design an active tool post and place it on the X-Y stage. The toolpost would have small range but high accuracy of positioning compared to the lead-screw drive. Almost all of the previous designs of fast tool servo are actuated by piezo-electric actuators although the sensing, mechanical design and control algorithms vary [Patterson and Magrab, 1985; Hara et al., 1990; Okazaki, 1990]. The reason is that the piezo-electric actuator has many advantages [King, 1990] such as: 1. there is no backlash and friction in the actuator, 2. the actuator can produce large forces, and 3. it has a small size and is easy to control. However, there are also some real-world imperfections such as: 1. hysteresis behavior, 2. drift in time, 3. temperature dependence, and 4. the finite stiffness of the actuator.

The CMAC idea was first introduced by Albus [1975] for robotic manipulators control. The idea is to replicate the structure and functions of various cell and fiber in the human cerebellum. It was later implemented on industrial robotic manipulators control by Miller et al. [1987]. Cetinkunt and Donmez [1993], Larson [1993] and Larson et al. have shown that CMAC neural network control algorithm had the potential to learn and compensate the errors caused by friction in high precision motion control. A piezo-electric actuated fast tool servo is presented in this paper. CMAC neural network control is implemented as the control algorithm to compensate the errors caused by the non-linearity of the actuator, and its performance will be compared with the industrial standard proportional-integral-derivative (PID) control algorithm. The design and the components of the fast-tool-servo are described in the next section. Open loop dynamic characteristic is discussed in section 3, followed by the real-time control algorithms in section 4. The experimental results and discussion are presented in section 5, followed by conclusions.

DESCRIPTION OF THE FAST TOOL SERVO DESIGN

The toolpost is designed as a parallel leaf spring mechanism (Fig.1). The piezo-electric stack motion is converted to tool displacement through a leaf spring design which is kinematically equivalent to a four-bar linkage. The good points of the mechanism are that it is small, and it has very high stiffness in the vertical direction. The capacitance type gap sensor for measuring the displacement of the toolpost is placed behind the toolpost. The control system block diagram is shown in figure 2. The detailed characteristics of each components of the control system are listed below.

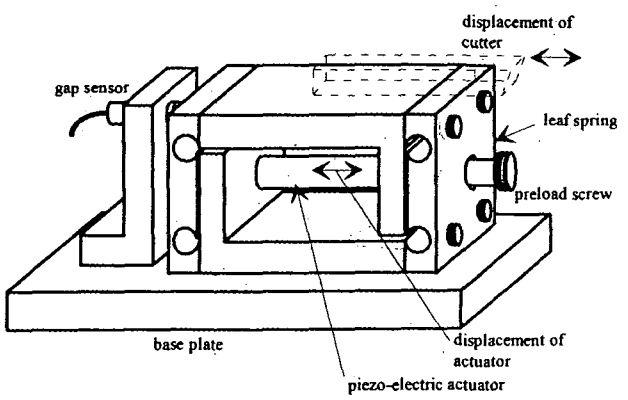

Fig.1 - Leaf spring mechanism with piezo-electric actuator

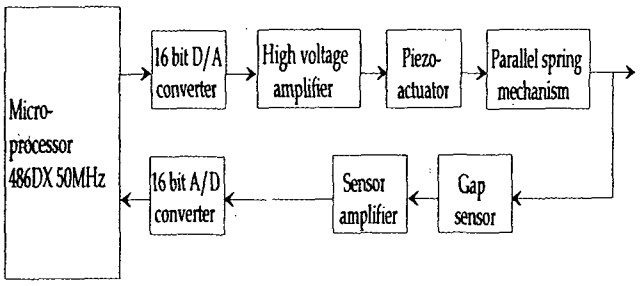

Fig.2 - PC-computer based control system

Piezoelectric actuator:

Nominal expansion at +100 V	15 μm
Maximum pushing force	1000 N
Maximum pulling force	100 N
Mechanical preload	100 N
Stiffness	55 N/μm
Electric capacitance	1.8 μF
Resonance frequency	18 kHz
Maximum hysteresis width	15 %
Total length	32 mm

Gap sensor:

Nominal standoff	4 mils (101.6 μm)
Range	2 mils (50.8 μm)
Sensitivity	10 V/mils (0.3937 V/μm)
Resolution	0.77 nm
Linearity	0.060%
Bandwidth	10 kHz

High voltage amplifier:

Input voltage	0 V to +10V
Output voltage	0 V to +100 V
Maximum current	0.2 A

Controller interface devices:

A/D Input channels	8 differential
D/A Output channels	2 independent
Resolution	16 bits
Maximum sample rate	47.6 ksamples/s
Timer	time interrupt circuit (hardware timer)

OPEN LOOP DYNAMIC CHARACTERISTICS OF THE TOOL POST

Understanding the open loop characteristics of a dynamic system is necessary for the design of a proper closed loop controller. The hysteresis, static stiffness and frequency response of the toolpost are discussed below.

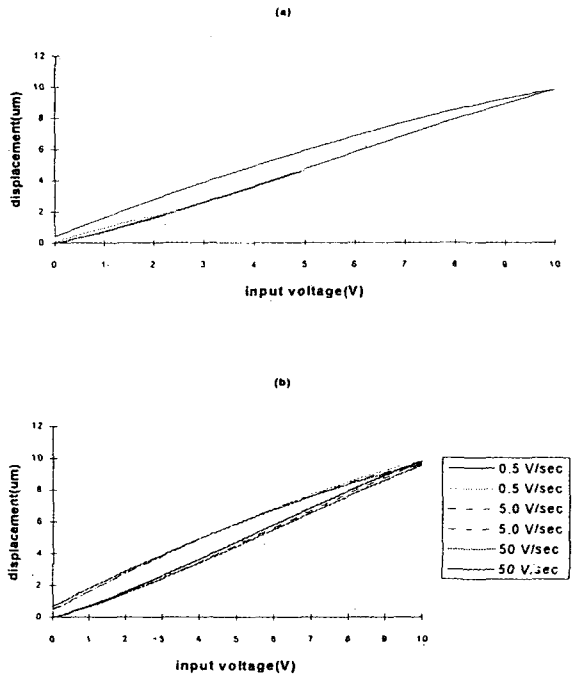

Fig.3 - Hysteresis characteristics of the toolpost: (a) displacement versus input magnitude, (b) displacement versus input voltage for various input voltage rates

Fig.3.a shows the hysteresis curve for various input voltage magnitudes sent to the high voltage amplifier (Fig.2). It is clear that hysteresis width largely depends on the input voltage magnitude. For small input magnitude, hysteresis width is small, and it increases with the increase of the input magnitude. The influence of input rate of change on the hysteresis curve is illustrated in Fig.3.b. Input voltage rate of change does not have much effect on the hysteresis width. Only slight increase of hysteresis width was observed with the increasing input voltage rate of change. Figure 4 shows the displacements of the parallel leaf spring against various external force magnitudes. The static stiffness of the mechanism is determined from the graph to be 9.09 N/μm. The displacements of the mechanism under 100 N preload against various forces is also shown in Fig.4. The preload is applied by the preload screw on the leaf spring (Fig.1). The static stiffness of the mechanism including the actuator can be determined to be 24.6 N/μm, almost only half of the stiffness of the actuator itself. The drop of stiffness is caused by the deformation of the mechanical parts. It is also important to note that preload also significantly reduces the hysteresis of the piezo-electric actuator compared to non-preload case.

Fig.5. shows the Bode plot of the frequency response of the n loop system. Numerical random numbers were used as ıdo random noise input with a sampling rate of 5 kHz. The ıtation signal is sent to voltage amplifier through 16-bit D/A verter. The displacement of toolpost is measured by sampling gap sensor signal through 16-bit A/D converter. MATLAB ıal processing software was used to implement discrete rier Transform and obtain Bode plot of the open loop uency response from the samples of I/O. From Fig.5, the ıral frequency of the mechanism was determined to be roximately 1.25 kHz, and the system has small damping ch is obvious from the large overshoot of the magnitude plot.

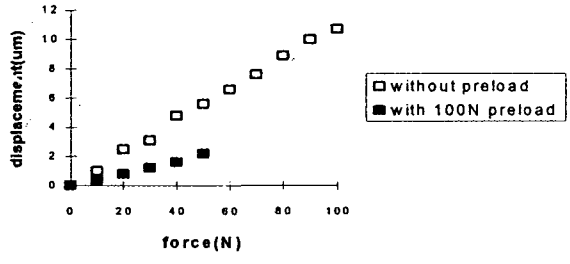

Fig.4 - Static stiffness of the toolpost

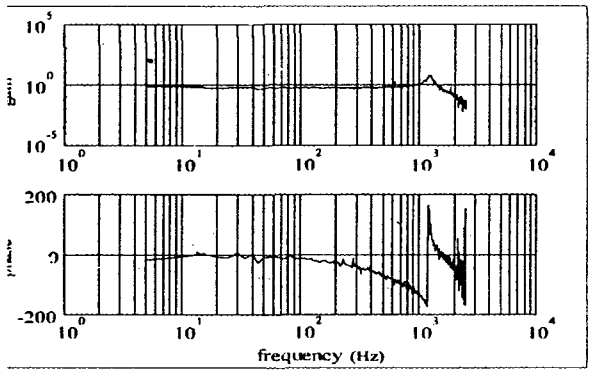

g.5 - Bode plot of the frequency response of open loop system

NTROL ALGORITHMS

Two different classes of control algorithms are studied in the -time control experiments: 1. proportional-integral-derivative troller (PID), 2. cerebellar model articulation controller fAC) neural network based control algorithm. The following lel of the toolpost was used as a guidance in the design of trol algorithm structure as well as tuning of the control ıithm parameters. Forces exerted by piezo-electric actuator be modeled as the forces generated by a force generator as in 6, and have the magnitude of $k \cdot y$, where y is the free ansion of the PZT material due to the input voltage. M is the s of the system including the actuator and the leaf spring hanism, c is the damping, and k is the stiffness.

The free expansion of the actuator, y, depends on the ırization of the PZT material , and is not exactly proportional he input voltage. Due to the hysteresis, the amount of the actuator displacement at a given voltage depends on whether it was previously operated at a higher or lower voltage (Fig. 3). The dynamic equations of the model shown in Fig. 6 is a text book example standard second order system with input-output transfer function

$$\frac{X(s)}{Y(s)} = \frac{\omega_n^2}{s^2 + 2\zeta\omega_n s + \omega_n^2}, \qquad (1)$$

where $\omega_n = \sqrt{\frac{k}{M}}$ and $\zeta = \frac{c}{2\sqrt{kM}}$.

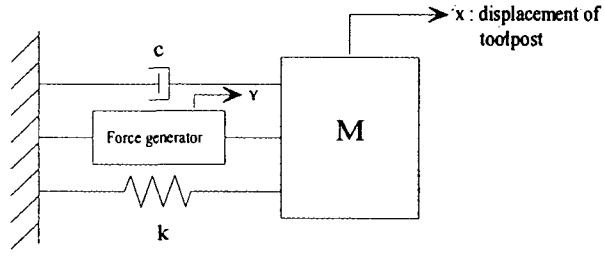

Fig.6 - Dynamic model of tool post with force generator

PID Control Algorithm:

Figure 7 shows the block diagram of the PID control algorithm implemented in real-time and used for comparisons to evaluate the performance of the CMAC neural network control.

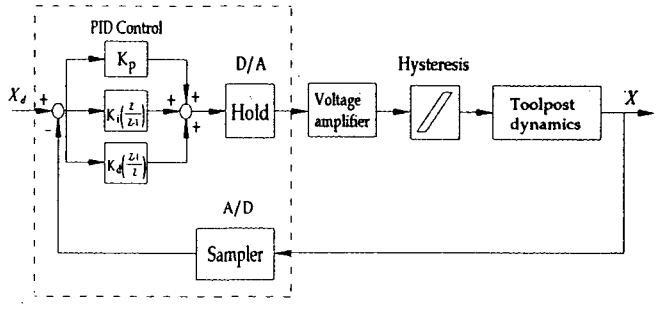

Fig.7 - Block diagram of the system with PID control algorithm

CMAC Neural Network Control Algorithm:

CMAC is essentially a table look up algorithm which is adaptive because it can modify the contents in the table by using learning algorithm. It has generalization capability due to the distributed storage of information. Fig.8 shows a block diagram describing the function of CMAC. CMAC has two basic components as:

1. mapping an input space into a finite number of memory location,

2. a learning algorithm based on the difference between a reference and CMAC response.

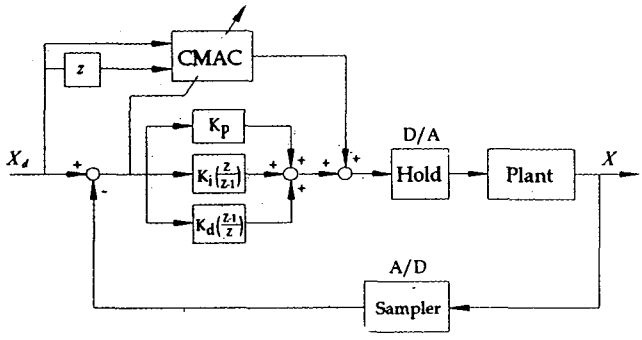

Fig.8 - Block diagram of the system with CMAC & PID control

From Fig.8, the function of CMAC is as follows:

Step 1: sample the input vector which may contain both desired and feedback information,

Step 2: find corresponding memory locations for that input vector using mapping algorithm,

Step 3: response from CMAC is then the summation of the contents of these active memory locations,

$$\hat{f}(s) = \sum_{i=1}^{n_g} w \quad , \tag{2}$$

where w_i is the content of n_g memory locations determined by the mapping algorithm in step 2,

Step 4: compare CMAC response with desired response, and modify or update the contents of the active memory locations by the learning algorithm,

$$w_i = w_i + \beta(f(s) - \hat{f}(s)) \quad , \tag{3}$$

where β is the learning rate.

Step 5: repeat until a learning accuracy criteria is satisfied.

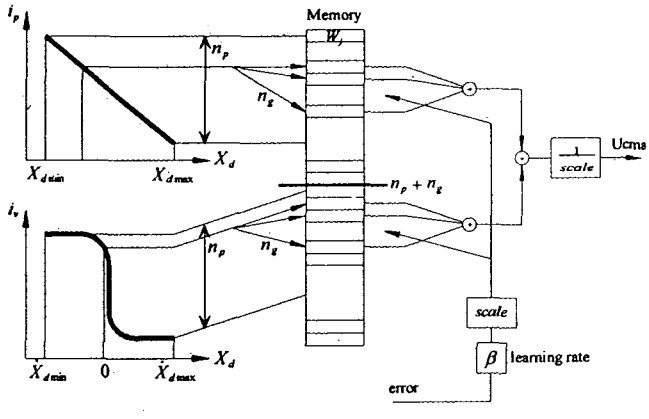

Fig.9 - Memory mapping of CMAC

The details of each step of CMAC algorithm is discussed next. The input space of this CMAC scheme is composed of two input components, position and velocity. Figure 9 shows the mapping algorithm (Step 1 and Step 2). The position memory locations are mapped linearly according to

$$I_p = \left(\frac{X_d - X_{\min}}{X_{\max} - X_{\min}} \right) * n_p \quad ,$$

and velocity memory locations are mapped nonlinearly as:

$$I_v = \left\{ sign\ (\dot{X}_d) \left(1 - \frac{1}{1 + \sqrt{\frac{|\dot{X}_d|}{\dot{X}_{dcr}}}} \right) \left(\frac{n_p}{2} \right) \right\} + \frac{n_p}{2}$$

CMAC response (Step 3) is determined from,

$$U_{CMAC} = \frac{\left(\sum_{j=I_p}^{I_p + n_g - 1} W_j + \sum_{j=n_h + I_v}^{n_h + I_v + n_g - 1} W_j \right)}{scale} \quad ,$$

where $n_h = n_p + n_g$.

And finally, learning algorithm (Step 4) is based o tracking error which modifies the content of currently memory locations by the following algorithm

$$W_j = W_j + (\beta * scale * error) \quad ,$$

for $j = I_p$ to $I_p + n_g - 1$,

and $n_h + I_v$ to $n_h + I_v + n_g - 1$.

The total memory size is $2 * n_h = 2 * (n_p +$ where n_p is the resolution of input mapping, and n_g generalization size .

REAL-TIME CONTROL EXPERIMENT RESULTS AN DISCUSSIONS

Performance of the toolpost control system is tested c large number of experiments. Only a few selected results w presented here to illustrate the capabilities of the toolpost two different types of control algorithms. From the con simulations, the proportional and the derivative gains di improve the quality of responses of the PID control system. proportional control action and the derivative control action then removed from the PID control scheme. For the C control system, CMAC algorithm is added parallel to the in controller.

Evaluation of stroke and resolution of toolpost:

A sinusoidal motion with 5 Hz frequency with va amplitudes were applied to the closed loop system w controller. Integral gain of 500 V/μm-s and 1 kHz samplin were used for all these experiments. In Fig. 10.a, the tra performance of the toolpost for almost the whole motion ra shown under integral control. In order to test the precision position control, the amplitude of reference input was decr to 0.002 μm (2 nm). Fig. 10.b shows the response of the s to 2 nm amplitude input. For very small amplitude of refe

out of 2 nm which is almost as same as the magnitude of noise, sponse tracked the reference input fairly well. It can be ncluded that the precision of the closed loop control system is out 2 nm.

acking accuracy of closed loop system under I and MAC control:

The integral gain, 500 V/μm-s, was used in the integral ntrol system (Fig. 7). The values of the integral gain of 100 μm-s and the learning rate (β) of 0.1 were used in the CMAC d I control system (Fig. 8). Sampling rate of 1 kHz was used in th systems. Tracking accuracy was tested using two different mmand signals:

1) 5 Hz sinusoidal signal with 100 nm magnitude,

2) 5 Hz square wave with 100 nm magnitude.

Integral control has the same tracking performance during ery cycle (Fig. 11a, 12a). About 10 msec delay in the tracking der I control is apparent in both figures. CMAC control rforms poorly during the first few cycles since the learning has t converged yet. After about five cycles or one second, CMAC able to learn the dynamic characteristics of the system, and proves tracking accuracy (Fig. 11b, 12b).

sturbance rejection:

Fig.13 shows the influence of disturbance on the response der the I control and to the CMAC control. A 5 Hz pseudo p periodic input with 0.1 μm amplitude was used as the ference for both systems. Disturbance introduced to the periment by removing of a weight initially hanged on the olpost under the gravity pull. The integral control alone has tter disturbance rejection ability than CMAC control has. The ason is that this CMAC design does not have any learning actions to learn the effect of the disturbance forces, and the lue of the integral gain used in the CMAC control system is aller than one used in the integral control system.

ONCLUSIONS

A high precision, high bandwidth toolpost is designed and bricated using piezo-electric actuation. The open loop namics of the toolpost is experimentally characterized. The osed loop control performance under a PID control and CMAC ural network control algorithms are tested and compared. The olpost has about 10 μm motion range by design. Using a pacity gap sensor, and IBM-PC/486 with 16-bit A/D and D/As control hardware, steady state positioning accuracy of 2 nm is hieved. The CMAC neural network control improved tracking curacy compared to the PID control. The steady state sitioning accuracy were essentially same under both control gorithms. The reason is that at the steady-state the main miting factor for positioning accuracy is the sensor resolution. ie disturbance rejection capability of CMAC control system uld be improved by training the CMAC with the disturbance. a alternative way to achieve this is to design a disturbance estimator, and train the CMAC with the estimated disturbance as well as the desired position and velocity.

REFERENCES

Albus, J., *Brains, Behavior, and Robotics,* BYTE Books, 1981.

Albus, J., "A new approach to manipulator control: The Cerebellar Model Articulation Controller (CMAC)," *ASME Journal of Dyn. Syst. Mea. and Control*, Sept. 1975, pp 220-227.

Albus, J., "Data storage in the Cerebellar Model Articulation Controller (CMAC)," *ASME Journal of Dyn. Syst. Mea. and Control*, Sept. 1975, pp 228-233.

Cetinkunt, S., Donmez, A., "CMAC learning controller for servo control of high precision machine tools," *Proceedings of the American Control Conference*, June 1993, San Francisco, CA.

Evans, C., "Cryogenic diamond turning of stainless steel," *CIRP Annals*, 1991, Vol.40, No.1, pp 571-575.

Hara, Y., Motonishi, S., Yoshida, K., "A new micro-cutting device with high stiffness and resolution," *CIRP Annals*, Vol. 39 No.1, pp 375-378, 1990

Keauskopf, B, "Diamond turning: Reflecting demands for precision," *Manufacturing Engineering*, May 1984, pp 90-100.

King, T.G., "Piezo-electric ceramic actuators: A review of machinery application," *Precision Engineering*, 1990, Vol.12, No.3, pp 131-136

Larsen, G., "CMAC neural network control for high precision machining," M.S. Thesis, University of Illinois at Chicago, 1993.

Larsen, G., Cetinkunt, S., Donmez, A., "CMAC neural network control for high precision motion control in presence of large friction," *ASME Journal of Dyn. Syst. Meas. and Control*, to appear.

Miller, W.T., Glanz, F.H., Kraft, L.G., "Application of a general learning algorithm to the control of robotic manipulators," *Int. Journal of Robotic Research*, Vol. 6, No. 2, pp 84-98, Summer 1987.

Okazaki, Y., "A micro-positioning toolpost using a piezo-electric actuator for diamond turning machines," *Precision Engineering*, 1990, Vol.12, No.3, pp 151-156.

Patterson, S.R., Magrab, E.B., "Design and testing of a fast tool servo for diamond turning," *Precision Engineering*, 1985, Vol.7, No.3, pp 123-128.

Ramsey, K.A., "Effective measurements for structural dynamics testing (part I)," *Sound and Vibration*, Nov. 1975, pp 24-35.

Ramsey, K.A., "Effective measurements for structural dynamics testing (part II)," *Sound and Vibration*, April 1976, pp 18-31.

Ueda, K., Amano, A., Qgawa, K., Takamatsu, H., Sakuta, S., "Machining high precision mirror using newly developed CNC machine," *CIRP Annals*, 1991, Vol 40, No.1, pp 554-558.

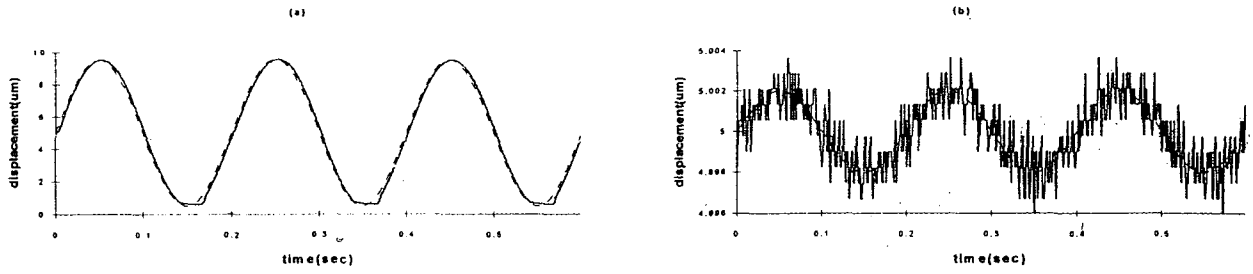

Fig.10 - Tracking response of I control system to 5 Hz sinusoidal input with
(a) 4.5 μm amplitude, (b) 2 nm amplitude

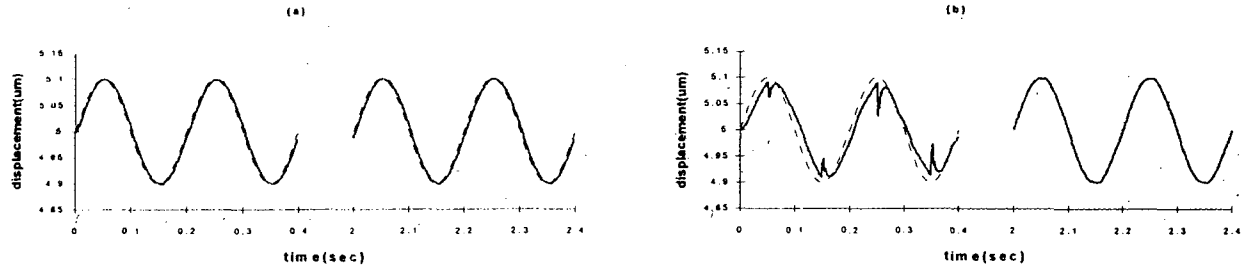

Fig.11 - Tracking response to 5 Hz sine wave input with 0.1 μm amplitude of
(a) I control system, (b) CMAC& I control system

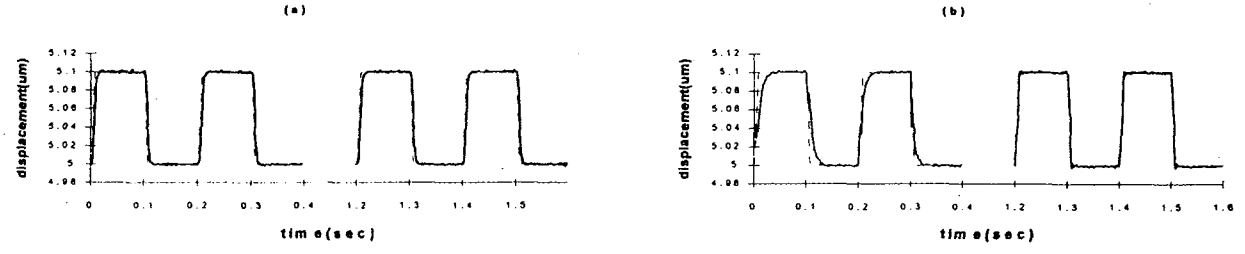

Fig.12 - Tracking response to 5 Hz square wave input with 0.1 μm amplitude of
(a) I control system, (b) CMAC& I control system

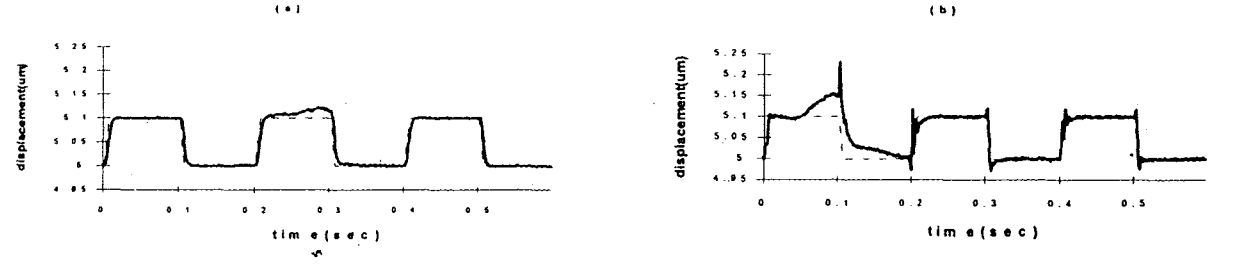

Fig.13 - Disturbance rejection of
(a) I control system, (b) CMAC& I control system